

Intracellular Trafficking and Uptake of Hyaluronan-Doxorubicin Conjugates in Vitro

By

ADEL

ALHOWYAN

Submitted to the graduate degree program in pharmaceutical chemistry and the Graduate Faculty of the University of Kansas in partial fulfillment of the requirements for the degree of Master of Science.

Chairperson: Dr. Laird Forrest

Dr. Jeff Krise

Dr. Teruna Siahaan

Date Defended: 23/7/2012

The Thesis Committee for ADEL ALHOWYAN
certifies that this is the approved version of the following thesis:

**Intracellular Trafficking and Uptake of Hyaluronan-Doxorubicin
Conjugates in Vitro**

Chairperson: Dr. Laird Forrest

Date approved: 23/7/2012

Abstract:

The purpose of this study was to determine the mechanism of uptake and release of doxorubicin from HA nanoparticle. We used human head and neck squamous cell carcinoma MDA-1986 as a model cell line. MDA-1986 was imaged after incubation with HA-DOX (NPs), doxorubicin, HA-CY7 or HA-DOX-CY7 at 15 minutes, 1, 6, 24, and 48 hours' time points using an inverted fluorescence microscope. Also, the cell nucleus was stained with DAPI stain, and the cells were imaged after incubation with HA-DOX conjugates, doxorubicin, HA-CY7 or HA-DOX-CY7 for 6 hours. Furthermore, the lysosomes were stained to determine if the lysosomal pathway is the major degradation pathway of the nanoparticles and the carrier. To determine the internalization mechanism, four inhibition conditions were used: excess HA to block HA receptors, anti CD44 antibody (Hermes-1) to block the CD44 receptor, chlorpromazine to inhibit clathrin mediated endocytosis, and reduced temperature of 4°C. The fluorescence intensities of the cells co-incubated with the nanoparticle or the carrier with different inhibitors were compared using the inverted fluorescence microscope. The quantitative analysis of cells treated with HA-DOX and co-incubated with different inhibition conditions (10 mg/mL HA, chlorpromazine, Hermes-1 and 4°C) showed significant decrease in the fluorescence intensity except in cells pretreated with 5 mg/mL HA. Also, the quantitative analysis of cells treated with HA-CY7 and co-incubated with different inhibition conditions (excess HA, chlorpromazine and Hermes-1) showed significant decrease in the fluorescence intensity. However, the quantitative analysis of cells treated with free doxorubicin or HA-DOX-CY7 showed significant decrease in the fluorescence intensity in only cells pretreated with 25- μ M chlorpromazine or cells incubated at 4 °C. The suggested internalization mechanism of HA-DOX conjugates is an active transport mechanism mediated mainly by the CD44, one of the HA receptors, through a clathrin-dependent endocytic pathway. On the other hand, a sulfated-HA derivative has similar uptake profile as the parent HA-CY7, and it is mainly localized in the cytosol.

Acknowledgment:

This study was conducted at Pharmaceutical Chemistry Department, University of Kansas.

I would like to express my deep gratitude to my supervisor Dr. Laird Forrest for his patience and the excellent scientific guidance and support.

I would like also, to thank my committee members, all Forrest lab members for their cooperation, Dr. Krise to allow us to use the microscope and Randy for the training.

Finally, I would like to thank King Saud University and Saudi Arabia Government for financial support to continue the graduate study outside Saudi Arabia Kingdom in one of the famous school in the world, pharmaceutical chemistry department in the University of Kansas.

July, 2012

ADEL ALHOWYAN

Table of Contents

Abstract:.....	iii
Acknowledgment:.....	iv
List of figures and tables:	vi
Chapter 1: Introduction.....	8
1.1 Cellular drug uptake:	8
1.2 Nanoparticles and drug uptake:	8
1.3 Role of HA to improve drug uptake in cancers:	10
1.4 HA-doxorubicin conjugates:	10
1.5 Purpose of the study:.....	11
Chapter 2: Internalization and cellular distribution of doxorubicin and hyaluronic acid.....	12
2.1 Materials:.....	12
2.2 Method:	12
2.3 Synthesis of HA-DOX conjugates:	16
2.4 Results:	19
2.5 Discussion:	42
2.6 Conclusions:.....	43
Chapter 3: Internalization of Sulfated-HA-CY7 experiments	44
3.1 Method:	45
3.2 Results:	46
3.3 Discussion:	48
Chapter 4:	49
Future work:	49
References:.....	50

List of Figures and Tables:

Table 1: Concentrations used for each drug in cell trafficking experiments

Table 2: Blocking conditions and uptake pathways

Table 3: Concentration of each drug used in the inhibition and competition experiments

Figure 1: Fluorescence spectra of free DOX and free CY7 dye

Figure 2: Synthesis of hyaluronan–doxorubicin (HA–DOX) conjugates

Figure 3: Chemical structure of HA-CY7

Figure 4: Fluorescence micrographs of HA-DOX uptake at 15 minutes, 1, 6, 24 and 48 hours

Figure 5: Fluorescence micrographs of free doxorubicin uptake at 15 minutes, 1, 6, 24 and 48 hours

Figure 6: Fluorescence micrographs of HA-CY7 uptake at 15 minutes, 1, 6, 24 and 48 hours

Figure 7: Fluorescence micrographs of free CY7 uptake at 15 minutes, 1, 6, 24 and 48 hours

Figure 8: Fluorescence micrographs of HA-DOX-CY7 uptake at 15 minutes, 1, 6, 24 and 48 hours

Figure 9: Fluorescence micrographs of HA-DOX, HA-CY7, free doxorubicin and HA-DOX-CY7 cell uptake at 6 hours. The nuclei were costained with DAPI

Figure 10: Fluorescence micrographs of free DOX, HA-DOX, HA-CY7 and HA-DOX-CY7 cell uptake at 1 hours. The lysosomes were costained with lysotracker blue

Figure 11: Fluorescence micrograph of cells pretreated with Hermes-1 for 30 minutes

Figure 12: Fluorescence micrograph of cells pretreated with chlorpromazine for 30 minutes

Figure 13: HA-DOX fluorescence micrograph of cells pretreated with 5 mg/mL HA for 24 hours

Figure 14: Free DOX fluorescence micrograph of cells pretreated with 5 mg/mL HA for 24 hours

Figure 15: Free CY7 fluorescence micrograph of cells pretreated with 5 mg/mL HA for 24 hours

Figure 16: HA-CY7 fluorescence micrograph of cells pretreated with 5 mg/mL HA for 24 hours

Figure 17: HA-DOX-CY7 fluorescence micrograph of cells pretreated with 5 mg/mL HA for 24 hours

Figure 18: Comparison of the cellular fluorescence intensity of the HA-DOX

Figure 19: Comparison of the cellular fluorescence intensity of the HA-CY7

Figure 20: Comparison of the cells fluorescence intensity after 1 hour incubation with doxorubicin

Figure 21: Comparison of the cellular fluorescence intensity after 1 hour incubation with HA-DOX-CY7

Figure 22 : Comparison of the cellular fluorescence intensity after 1 hour incubation with HA-DOX, DOX and HA-DOX-CY7 at 37°C and 4°C

Figure 23: Chemical structure of Sulfated HA-CY7

Figure 24: Fluorescence micrographs of Sulfated-HA-CY7

Figure 24: Comparison of the cellular fluorescence intensity after 1 hour incubation with Sulfated HA-CY7

Chapter 1: Introduction

1.1 Cellular Drug Uptake:

There are many mechanisms of cellular drug uptake such as passive diffusion, carrier mediated transport, and pore transport. Small and lipophilic drugs usually pass the epithelial cell membrane by passive diffusion. The driving force for the passive diffusion is the concentration gradient. On the other hand, carrier-mediated transport utilizes specialized proteins to transport molecules. The specialized membrane proteins may pass the drug to the intracellular compartment by active transport, which is against the concentration gradient, or by facilitated diffusion, which is with the concentration gradient. Active transport is an energy consuming process because it is against the concentration gradient.

Endocytosis or engulfment of extracellular materials can be a major transport mechanism of large molecules that are more than 500 Da. It can be divided into two types; pinocytosis and phagocytosis. Pinocytosis is the invagination and formation of an inward channel, and it is a non-specific process. However, phagocytosis is a specific process for some specialized cells known as reticuloendothelial cells. On the other hand, very small hydrophilic molecules such as water can pass through the small pores in the cell membrane. These small pores are approximately 0.4 nm in diameter, but most drug molecules are larger than 1 nm in diameter. So, there is more than one mechanism for drugs or molecules to transport inside the cells. Some of them require energy and the mechanism of transport depend on size, molecular weight and solubility of the drug (1).

1.2 Nanoparticles and drug uptake:

Nanoparticles are complex systems with a nanometer scale from 10 to 100 nm, consisting of an active ingredient, such as drug or biomarker, and a carrier. This complex

system can be utilized for therapy, diagnosis or both as a theragnostic. The goals of using nanotechnology in the drug delivery are: increase in specificity, reduction in toxicity, and quicker development of a safe and efficacious formulation. However, there are many challenges in the fields of drug delivery and nanotechnology to design and produce a new active formulation. Some of these challenges are drug release and encapsulation, physical and chemical stability, distribution and targeting of the drug, and in vivo activity. So, the formulator should have broad physical, chemical and biological knowledge to succeed in developing a new formulation (2).

The fate of nanoparticles inside the cells is important. Degradation of the particles after intracellular uptake generally occurs in endosomes or lysosomes (2). The encapsulated drug inside the nanoparticles should reach the cytosol or the site of action inside the cells to be active. Nanoparticles with a particle size of about 20 nm could be taken up by cells without contribution of the endocytosis process (6). Surface charge of nanoparticles may have a contribution in the localization of the nanoparticles in the cells. For example, gold nanoparticles with a pegylated surface can be efficiently internalized in the cytosol and finally localized in the nucleus (7). Also, escape from endosomes to the cellular cytoplasm was found with PLGA nanoparticles. In contrast, polystyrene nanoparticles remained in the endosomal compartment and did not reach the cytosol. The hypothesis was that escape of PLGA nanoparticles from endosomes to the cytosol was due to the change in the surface charge from negative to positive in the PLGA nanoparticles. The PLGA NPs contained serum albumin, so they acquire a positive charge in the acidic pH such as endo-lysosomal vesicles (pH 4). Meanwhile they have a negative charge in physiological and alkaline pH, in contrast to polystyrene NPs which have a negative charge in all pH values. So, understanding the mechanism of cellular uptake and the fate of transport drugs inside the cell can improve the delivery and targeting of the drugs (8, 9).

1.3 Role of HA to improve drug uptake in cancers:

Hyaluronan (HA) is an anionic glycosaminoglycan widely distributed throughout the body. It is a biodegradable and biocompatible molecule with a wide molecular weight range from 10 to 10,000 kDa. In tissues, hyaluronan contributes in cell proliferation and migration, and it may be involved in cancer metastasis. There are different types of cell receptors of HA, including CD44, RHAMM and ICAM-1 receptors. The main cell surface receptor of HA is CD44. CD44 receptors mediate cell interaction with HA, and the binding of the two functions as an important part in various physiological events such as cell aggregation, proliferation, migration and endocytosis of HA which may cause degradation of HA(4). On the other hand, ICAM-1 receptors function as metabolic cell receptors for HA. When HA binds to these receptors, a cascade of events happen including endocytosis of HA which forms early endosomes, then fusion of these endosomes with the cellular lysosomes which contain enzymes that degrade the HA(4).

Hyaluronan has some intrinsic properties that make it a good delivery carrier for anticancer drugs. Hyaluronan is an endogenous compound and non-immunogenic at molecular weights above 10 kDa. Hyaluronan can form a large network at low concentration to entrap small anticancer drugs. In a tumor environment, there is overexpression of the CD44 receptor in tissues, which facilitates the uptake of the HA-anticancer conjugates by cancer cells. HA-anticancer conjugates can rapidly enter the tumor and accumulate within the tumor and could form an intra-tumoral drug depot after accumulation. So, using HA as a drug delivery carrier offers many advantages over other drug carrier systems for targeting cancer cells.

1.4 HA-doxorubicin conjugates:

Doxorubicin (DOX) is an anticancer drug used for treatment of various forms of cancer, including breast and ovarian cancers, sarcomas, pediatric solid tumors, Hodgkin's and non-

Hodgkin's lymphomas and multiple myeloma. Doxorubicin has several serious side effects, such as cardiac toxicity, which may limit its use. To decrease the side effects and toxicity of doxorubicin, different technologies can be used to reduce nonspecific tissue toxicity, such as polymeric micelles, antibody targeted carriers and polymeric conjugates (10, 17). Several HA–DOX conjugates have been reported that used peptide linkers, which had a considerable loss of anticancer activity (14-16). Our lab synthesized a new pH-sensitive, reversible hydrazone HA–DOX conjugate with potent anticancer activity against breast cancer cells in vitro and excellent cellular uptake and retention (10).

1.5 Purpose of the study:

The purpose of this study is to observe the effect of HA on DOX uptake after conjugation of DOX with HA. Furthermore, to determine which internalization mechanism is used by MDA-1986 cell line to uptake the HA-DOX nanoparticles, and the localization of both doxorubicin and HA by inverted fluorescence microscope. Also, we investigated and compared the uptake of a sulfated form of HA to the parent HA.

Chapter 2: Internalization and cellular distribution of doxorubicin and hyaluronic acid

2.1 Materials:

The 4', 6-Diamidino-2-phenylindole dihydrochloride (DAPI) stain was obtained from Fisher Scientific. CD44 monoclonal antibody (Hermes-1) was obtained from Thermo Fisher Scientific (Rockford). Poly-L-Lysine coated glass coverslips were obtained from BD Biosciences. Fisherfinest* Premium Plain Glass Microscope Slides (Size: 75 x 25mm) were obtained from Fisher Scientific. Doxorubicin was obtained from Bedford Laboratories. CY7 NHS ester dye was obtained from Lumiprobe. DMEM was obtained from Lonza. Hyaluronic acid was obtained from Lifecore Biomedical. Lyotracker blue was obtained from Invitrogen.

2.2 Method:

Cell line and cell culture conditions:

The cell line used was a human head and neck squamous cell carcinoma cell line, MDA-1986. Cells were grown in 75-cm² cell culture flasks in DMEM with 10 % fetal bovine serum (FBS) and 1% L-glutamine. When a confluent state was reached, cells were seeded in 12-multiwell plates (100,000-200,000 cells/well). Before imaging the cells, they were washed three times with phosphate buffer saline (PBS). Then, the coverslips were fixed on glass microscope slides.

Cellular uptake and trafficking experiments:

Doxorubicin has an excitation and an emission wavelength of 480 nm and 560 nm, respectively. HA does not have intrinsic fluorescence, i.e. it is non-fluorophorescent, so we conjugated HA to a laser dye CY7. CY7 dye has an excitation and an emission wavelength of 750 nm and 773 nm, respectively. Thus, the fluorescence signals of doxorubicin and HA-CY7

could be captured simultaneously using YFP and CY7 filter sets, respectively. We used the dual labeled molecules HA-DOX-CY7 to localize the carrier (HA) and the drug (doxorubicin) at the same time. DAPI staining was used to stain the nucleus, which has an absorption maximum at a wavelength of 358 nm and emission maximum at 461 nm (13). LysoTracker blue was used to stain the lysosomes, which has an absorption maximum at a wavelength of 373 nm and an emission maximum at 422 nm.

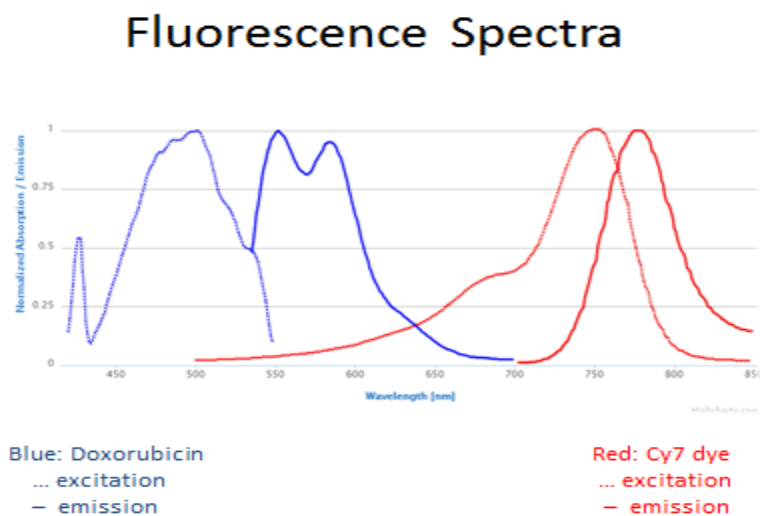


Figure 1: Fluorescence spectra of free DOX and free CY7 Dye.

The uptake of the HA-DOX, HA-CY7 and DOX-HA-CY7 was monitored with an inverted fluorescence microscope at 15 minutes, 1, 6, 24 and 48 hours. Furthermore, the cell nuclei were stained with DAPI staining (7.5 $\mu\text{g/ml}$) and the cells were imaged after 6 hours. To explore if the lysosomes are the major degradation pathway of the nanoconjugates and the carriers, the lysosomes were stained with LysoTracker blue (150-nM) and co-incubated with free doxorubicin, HA-DOX, HA-CY7 or HA-DOX-CY7 for one hour.

Table 1: The concentration used for each drug in cell trafficking experiments as follows:

Drugs	Concentration ($\mu\text{g}/\text{mL}$)
Doxorubicin	2
HA-DOX	1.4
HA-CY7	200 on HA basis
HA-DOX-CY7	50 on HA basis

Mechanism of cellular uptake:

To explore the internalization mechanism of the HA-DOX and trafficking across the plasma cell membrane, we studied four different inhibition conditions.

Table 2: Blocking conditions and uptake pathways.

Pathway	Inhibitor	Mechanism
HA receptor pathway	Hermes-1 (10 $\mu\text{g}/\text{mL}$)	Inhibits CD44-mediated uptake
HA receptor pathway	Excess HA (5 and 10 mg/mL)	Competitively inhibits HA uptake
Endocytosis	Chlorpromazine (25- μM)	Inhibits endocytosis by clathrin pathway
Endocytosis	4°C	Blocks energy-dependent internalization mechanisms (i.e. non-diffusion processes)

In chlorpromazine and Hermes-1 experiments, cells were incubated for 30 minutes with each inhibitor alone and then co-incubated with HA-DOX, free doxorubicin, HA-CY7 or HA-

DOX-CY7 for 1 hour. However, in HA competition experiments, cells were incubated with excess HA for 24 hours and then were incubated with HA-DOX, HA-CY7 or HA-DOX-CY7 for the 15 minutes, 1, 6, 24 and 48 hour time points. For 4°C experiments, cells were incubated for 30 minutes and then treated with HA-DOX, free DOX or HA-DOX-CY7 for one hour.

The fluorescence intensities for all four inhibition conditions were compared with non-treated cells using Image J program with this equation:

Corrected Total Cell Fluorescence (CTCF) = Integrated Density – (Area of selected cell x Mean fluorescence of background readings). Each assay was performed in triplicate or more and the statistical analysis was performed using student T test.

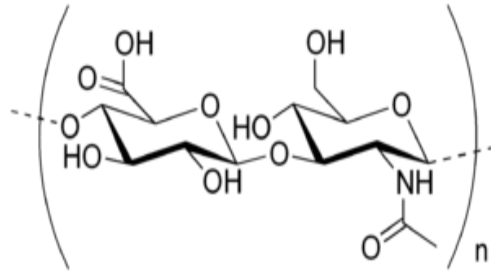
Table 3: concentration of each drug used in inhibition and competition experiments:

Drugs	Concentration (µg/mL)
Doxorubicin	2
HA-DOX	1.4
HA-CY7	400 on HA basis
HA-DOX-CY7	50 on HA basis

2.3 Synthesis of HA-DOX conjugates:

HA was conjugated to adipic acid dihydrazide (ADH) to facilitate the conjugation of HA to doxorubicin. HA (200 mg) with a molecular weight of 35 kDa was dissolved in 40 ml of ddH₂O with 436 mg of adipic acid dihydrazide and 48 mg of 1-ethyl-3-[3-(dimethylamino)-propyl]carbodiimide (EDCI). The pH was adjusted with 1-N HCl, and after 10 minutes the reaction was quenched with 0.1-N NaOH to reach pH 7. The solution was dialyzed for two days against ddH₂O. Then, the solution was lyophilized after filtering (0.2- μ m polysulfone membrane, Millipore). By using the ratio of ADH methylene protons to HA acetyl methyl protons, the degree of substitution was determined by ¹H-NMR in D₂O.

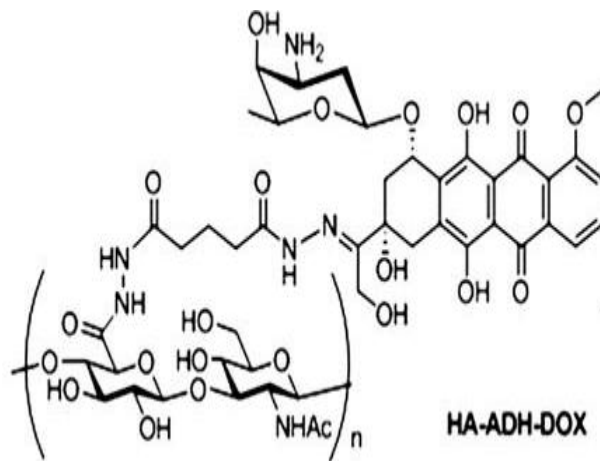
To conjugate DOX to HA, we allowed the ketone of DOX and the hydrazide side chain of HA-ADH to react and form a hydrazone. Briefly, 30 ml of 2-mM sodium phosphate buffer (pH 6.5) was used to dissolve 110 mg of HA-ADH. DOX·HCl (2 mL, 2 mg/mL) was added drop wise to 25 mL of H₂O. After adjusting the solution pH to 6.5 with 0.1-N NaOH, the solution was dialyzed against 2-mM sodium phosphate buffer (pH 7.8) until no further color change occurred. UV/Vis spectrophotometry at 480 nm was used to determine the degree of conjugation with a standard calibration curve (1–100 μ g/mL). Also, gel permeation chromatography was used to confirm the conjugation by equivalent elution time (GPC; Shodex HQ-806 M column, 0.8 mL/min 20-mM HEPES, pH 7.2) with refractive index and fluorescence detection (ex/em 480/590 nm) (10, 11, 12).



HA

↓ Adipic acid dihydrazide
EDAC pH 4.75

↓ DOX
phosphate buffer pH 6.5



HA-ADH-DOX

Figure 2: Synthesis of hyaluronan–doxorubicin (HA–ADH-DOX) conjugates

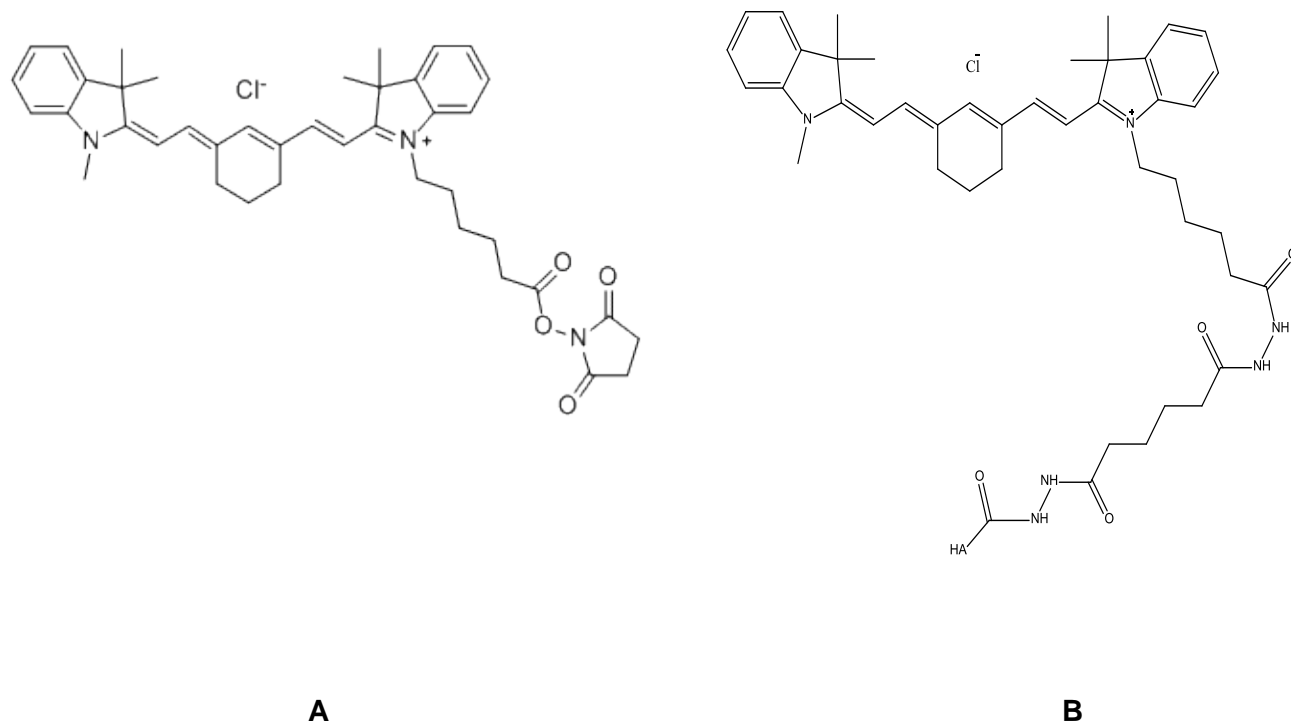


Figure 3: Chemical structures of: A) CY7 NHS ester and B) HA-ADH-CY7.

2.4 Results:

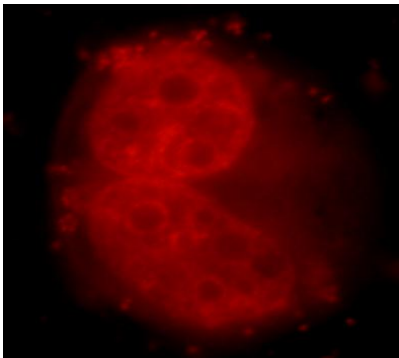
Intracellular Trafficking:

Free doxorubicin was rapidly up taken by cells, and it was mainly localized in the cell nucleus (figure 4). HA-CY7 and free CY7 mainly localized in the cytosol (figure 6 and 7). HA-DOX was found to be localized in two regions: in the nucleus and cytosol. After 15 minutes incubation, there was minimal internalization of HA-DOX. After 1 hour, there were two populations of cells. The majority of the cells with HA-DOX localized in the cytosol, and the other group of cells with HA-DOX localized in the nucleus. After 6 hours, HA-DOX mainly localized in the cell nucleus and remained there for 48 hours (figure 5). Also, HA-DOX-CY7 was found to be localized in two regions: the cytosol and cell nucleus. After 15 minutes, we could not distinguish between the doxorubicin signal and CY7 signal. After 1 hour to 48 hours, doxorubicin signal was found mainly in the cell nucleus, but CY7 signal was found in the cytosol. At 48 hours, there was a substantial amount of conjugates distribution in the cytoplasm where HA was bound to doxorubicin, suggesting that the HA-DOX conjugate released doxorubicin for an extended period of time (figure 8). The higher fluorescence intensity of free doxorubicin was found after incubating the cells with doxorubicin for 6 hours. Cells incubated with HA-DOX had higher fluorescence intensity after 24 hours. The difference between DOX and HA-DOX uptake was the earlier uptake of the free DOX compared to HA-DOX. Cells incubated with HA-CY7 had higher intensity after 24 hours while cells incubated with free CY7 had higher fluorescence intensity after 1 hour. The doxorubicin signal of the HA-DOX-CY7 was found the highest after 6 hours, while the CY7 signal was found the highest after 1 hour incubation.

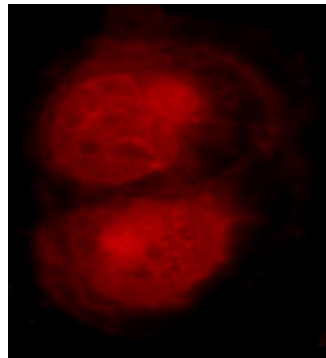
To further confirm the localization of the drug in the nucleus, we stained the nucleus with DAPI stain. We found both the CY7 signals of HA-CY7 and the dual labeled molecule HA-DOX-CY7 were localized in the cytosol. In contrast, the DOX signals of free DOX, HA-DOX and HA-DOX-CY7 were found in the cell nucleus co-localized with the DAPI stain (figure 9). On the

other hand, lysosomes were found to be co-localized with free DOX, HA-DOX, HA-CY7, HA-DOX-CY7 after one hour incubation with each molecule (figure 10).

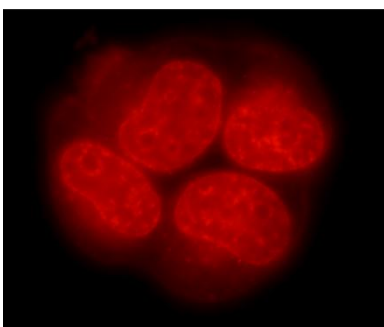
15 minute



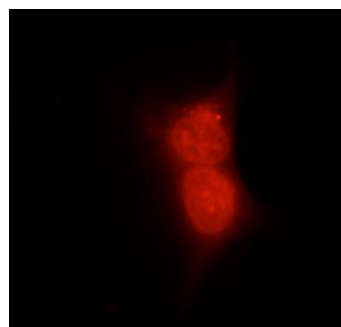
1 hour



6 hour



24 hour



48 hour

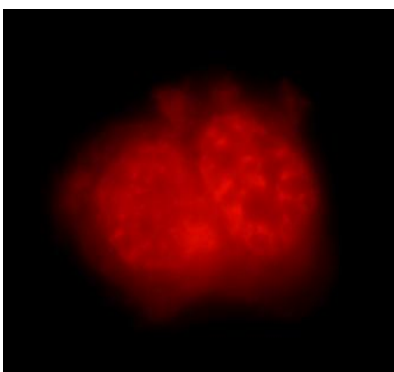
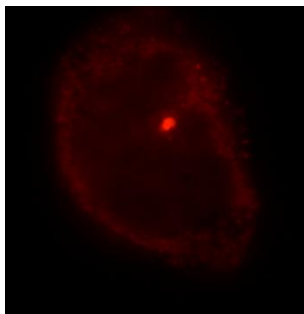


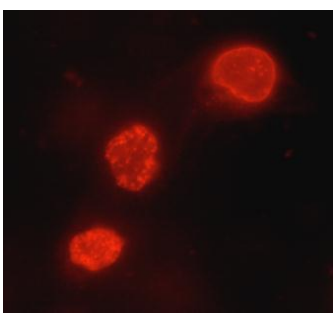
Figure 4 :

Fluorescence micrographs of free doxorubicin uptake at 15 minutes, 1, 6, 24 and 48 hours.

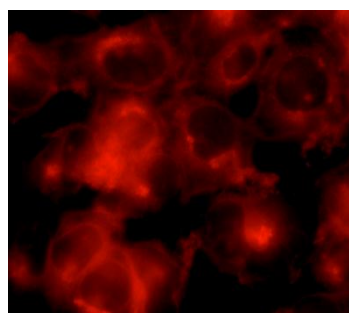
15 minute



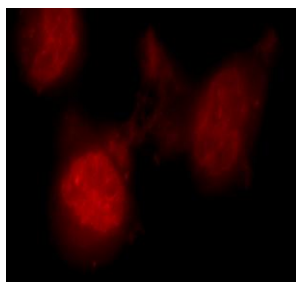
1 hour



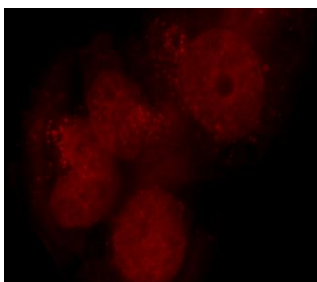
1 hour



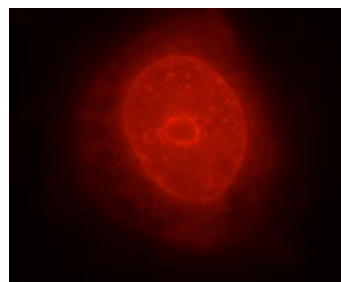
6 hour



24 hour



24 hour



48 hour

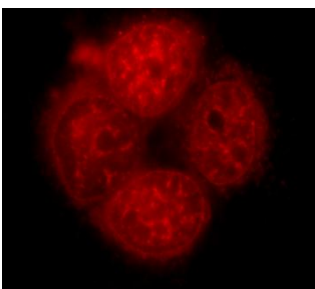
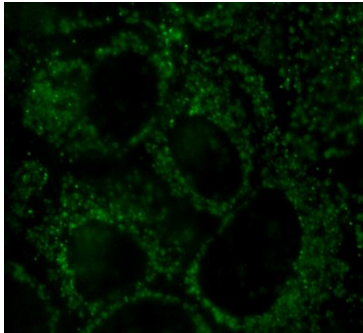


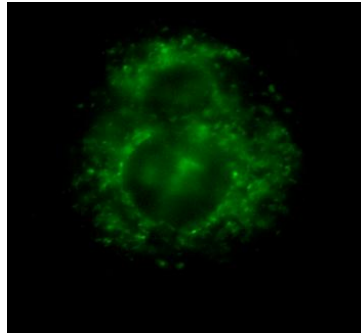
Figure 5 :

Fluorescence micrographs of HA-DOX uptake at 15 minutes, 1, 6, 24, 48 hours.

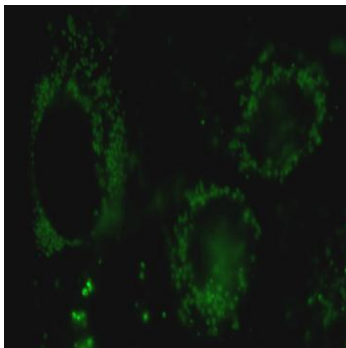
15 minute



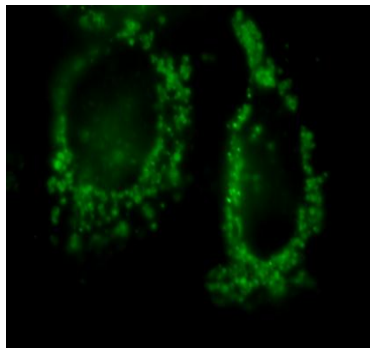
1 hour



6 hour



24 hour



48 hour

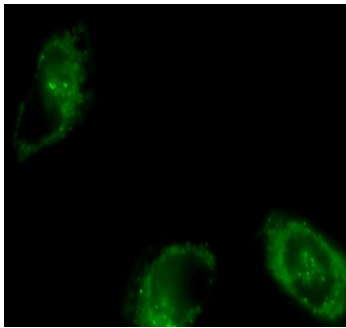
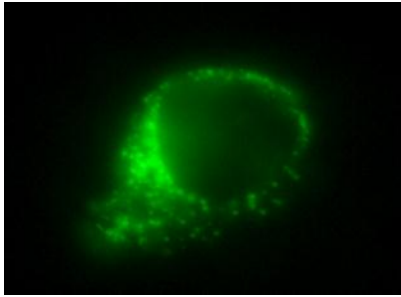


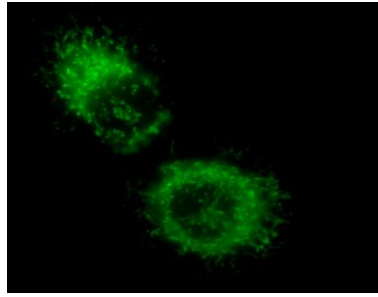
Figure 6:

Fluorescence micrographs of HA-CY7 uptake at 15 minutes, 1, 6, 24 and 48 hours.

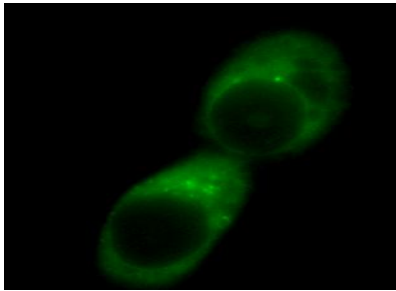
15 minute



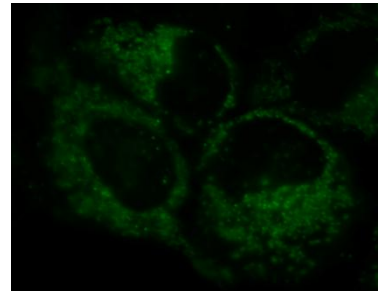
1 hour



6 hour



24 hour



48 hour

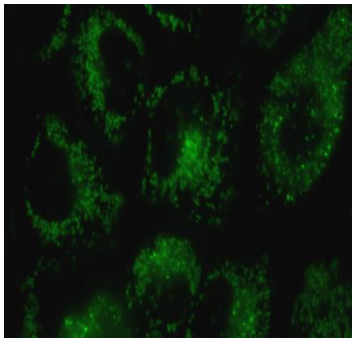
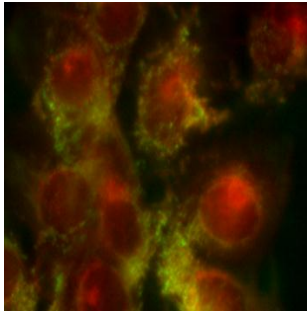


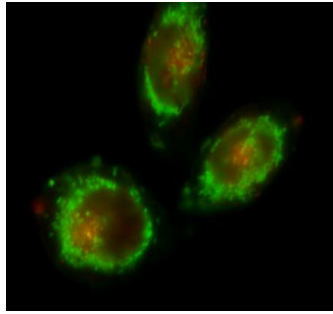
Figure 7:

Fluorescence micrographs of free CY7 uptake at 15 minutes, 1, 6, 24 and 48 hours.

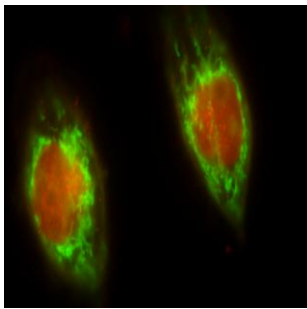
15 minute



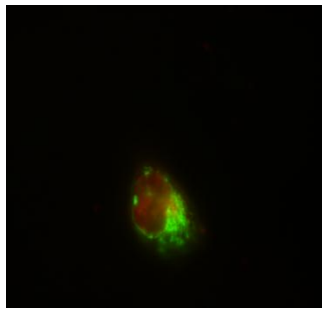
1 hour



6 hour



24 hour



48 hour

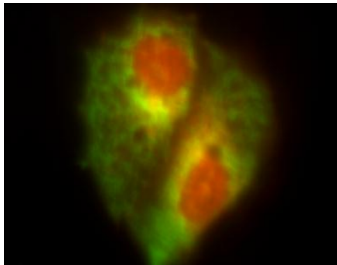


Figure 8:

Fluorescence micrographs of HA-DOX-CY7 uptake at 15 minute, 1, 6, 24 and 48 hours.

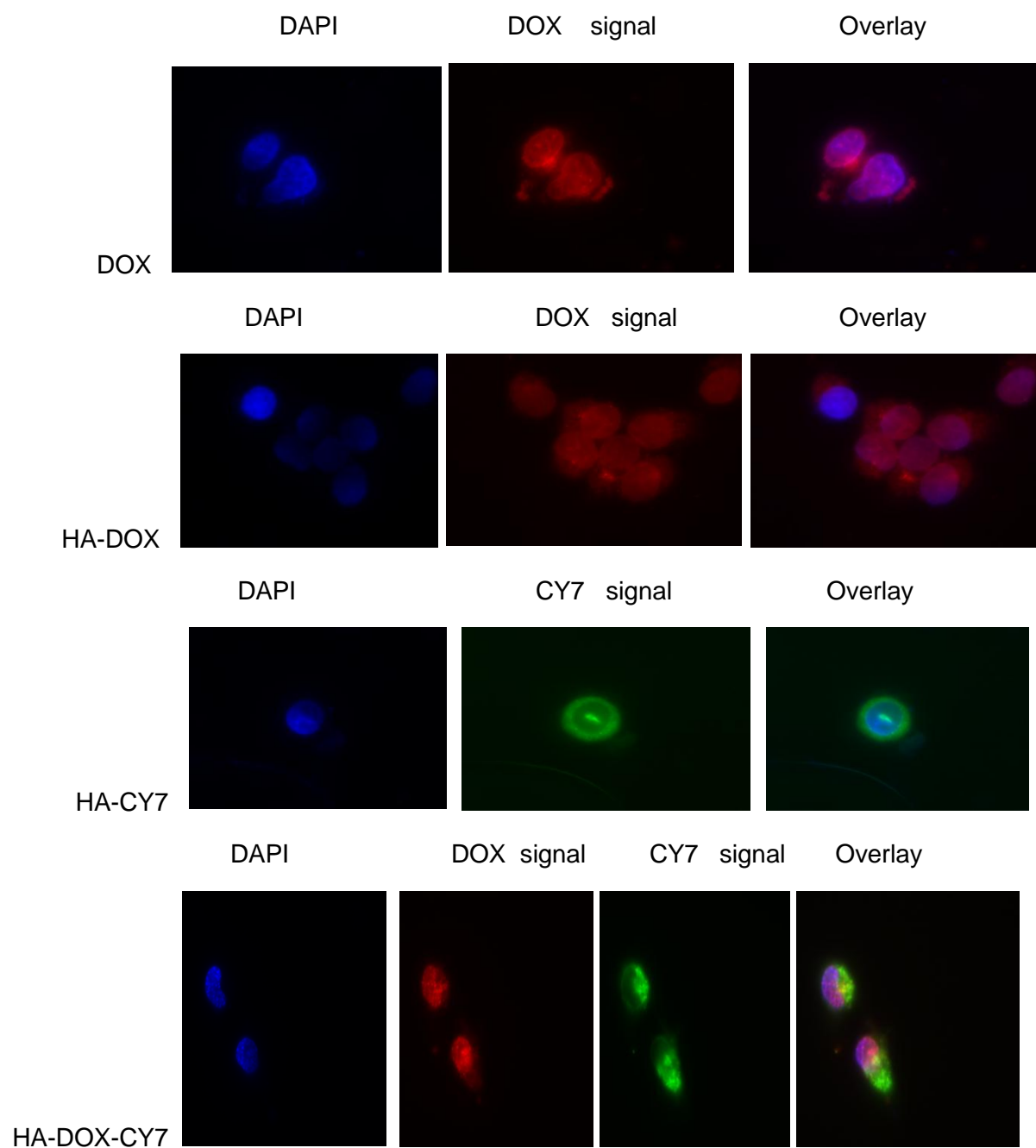


Figure 9:

Fluorescence micrographs of HA-DOX, HA-CY7, free doxorubicin and HA-DOX-CY7 cell uptake at 6 hours. The nuclei were co-stained with DAPI (blue), DOX signal (red) and CY7 signal (green).

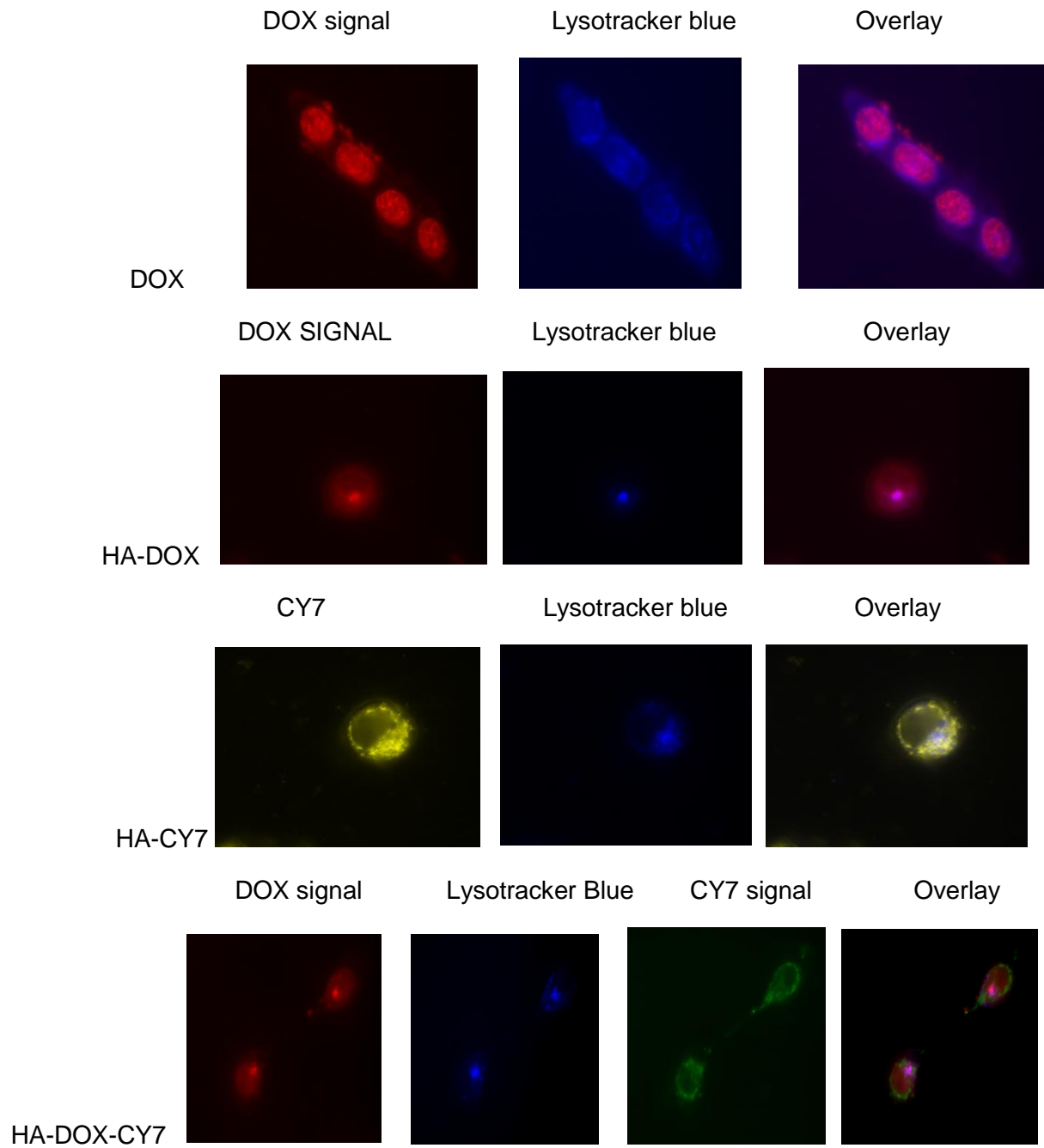


Figure 10:

Fluorescence micrographs of free DOX, HA-DOX, HA-CY7 and HA-DOX-CY7 cell uptake at 1 hours. The lysosomes were co-stained with lysotracker blue.

Mechanism of cellular uptake:

HA-Doxorubicin and Free Doxorubicin:

The quantitative analysis of cells treated with HA-DOX and co-incubated under different inhibition conditions (excess HA, chlorpromazine and Hermes-1) showed a significant decrease in the fluorescence intensity, except cells pretreated with 5 mg/mL HA. Furthermore, the cells treated with 25- μ M chlorpromazine had the lowest fluorescence intensity cells in the other treatment groups. The order of cell fluorescence intensities in all conditions were found as follows: HA-DOX alone, excess HA, Hermes-1 and chlorpromazine (Figure 18).

However, the quantitative analysis of cells treated with free doxorubicin showed a significant decrease in the fluorescence intensity only in cells pretreated with 25- μ M chlorpromazine (p value: 0.0018 figure 19).

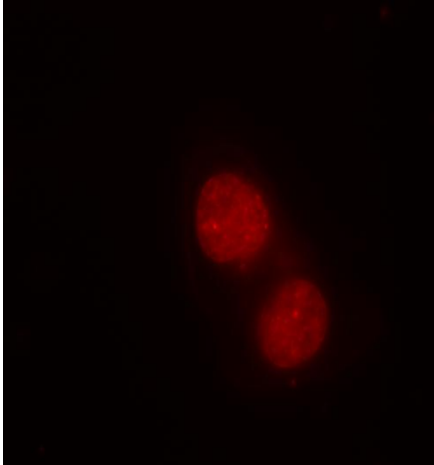
HA-CY7 and HA-DOX-CY7:

The quantitative analysis of cells treated with HA-CY7 and co-incubated under different inhibition conditions (excess HA, chlorpromazine and Hermes-1) showed a significant decrease in the fluorescence intensity in all inhibition conditions. Furthermore, the cells treated with 25- μ M chlorpromazine had the lowest fluorescence intensity compared to cells in the other treatment groups. The order of cell fluorescence intensities in all conditions was found as follows: HA-CY7 alone, excess HA, Hermes-1, and chlorpromazine (Figure 20). However, the quantitative analysis of cells treated with HA-DOX-CY7 showed a significant decrease in the fluorescence intensity only in cells pretreated with 25- μ M chlorpromazine (p value less than 0.05 figure 21).

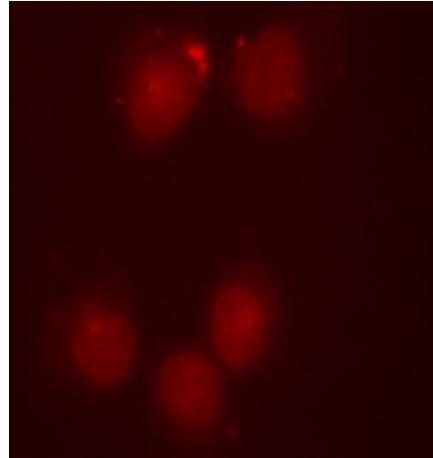
Temperature-dependent internalization studies:

As another way to inhibit the endocytosis process we compared the cellular uptake of HA-DOX, free DOX and HA-DOX-CY7 at 37°C and 4°C. We found that the cellular uptake of HA-DOX, free DOX and HA-DOX-CY7 significantly decreased at 4 °C compared to 37 °C (figure 22).

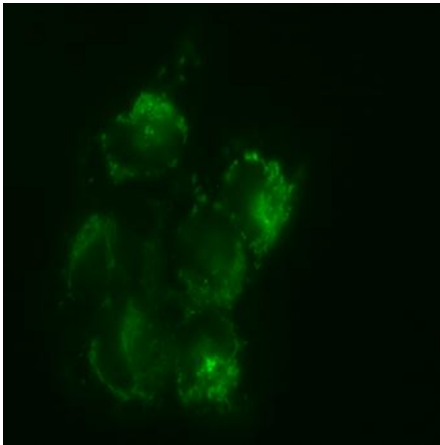
DOX



HA-DOX



HA-CY7



HA-DOX-CY7

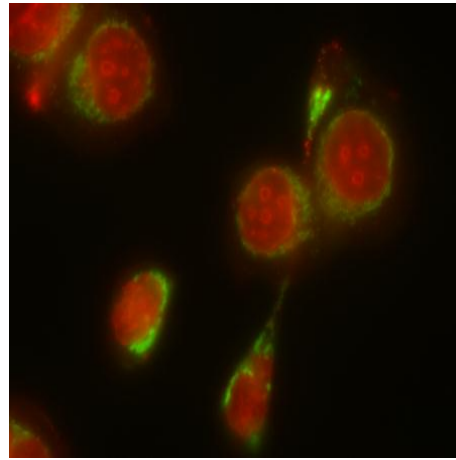
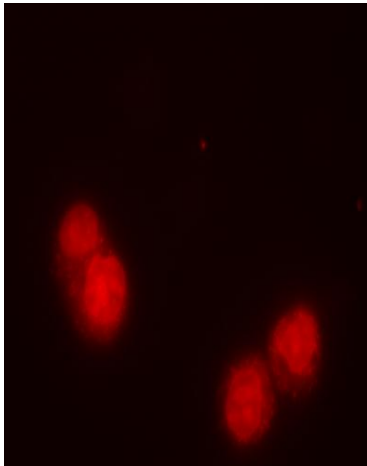


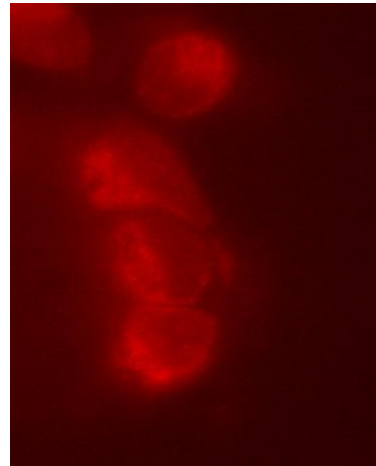
Figure 11:

Fluorescence micrographs of DOX, HA-DOX, HA-CY7 and HA-DOX-CY7 pretreated with Hermes1 for 30 minutes.

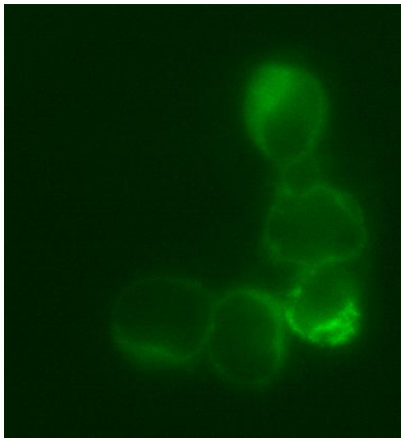
DOX



HA-DOX



HA-CY7



HA-DOX-CY7

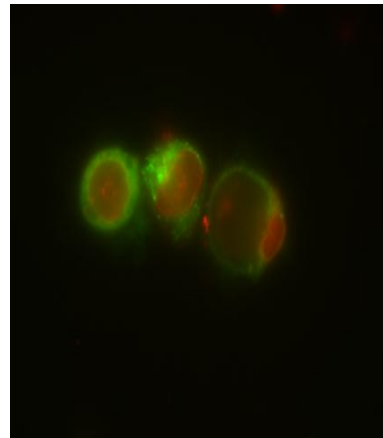
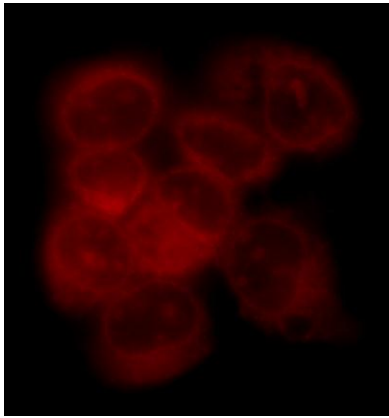


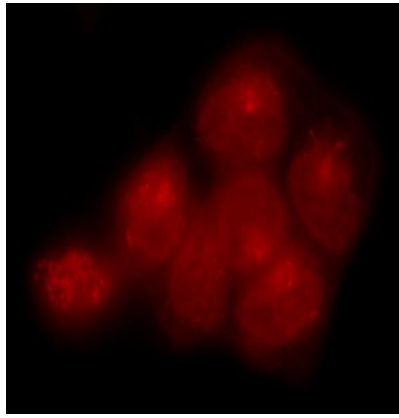
Figure 12:

Fluorescence micrographs of HA-DOX, HA-CY7 and HA-DOX-CY7 pretreated with chlorpromazine for 30 minutes.

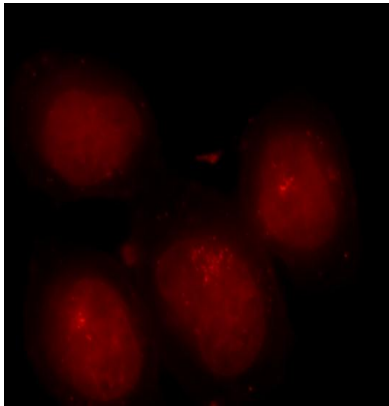
15 minute



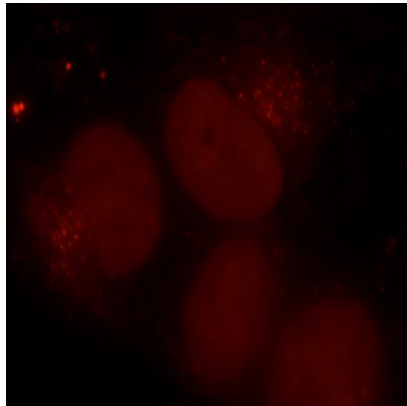
1 hour



6 hour



24 hour



48 hour

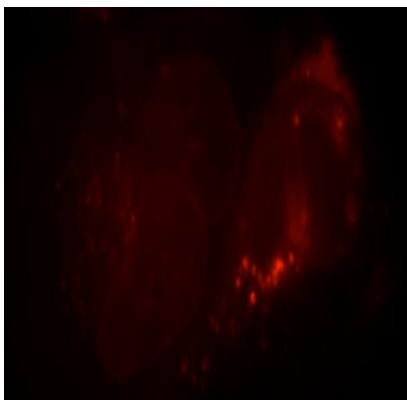
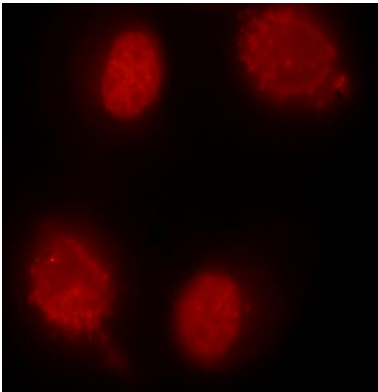


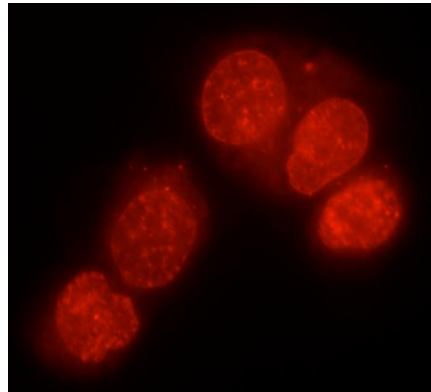
Figure 13:

HA-DOX fluorescence micrographs of cells pretreated with 5 mg/mL HA for 24 hours.

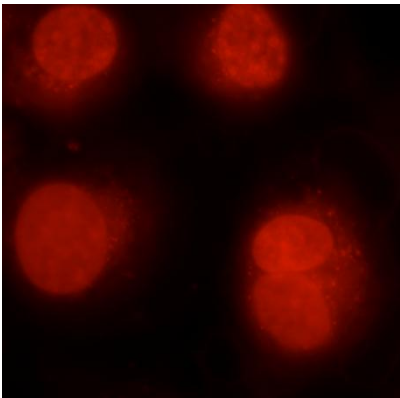
15 minute



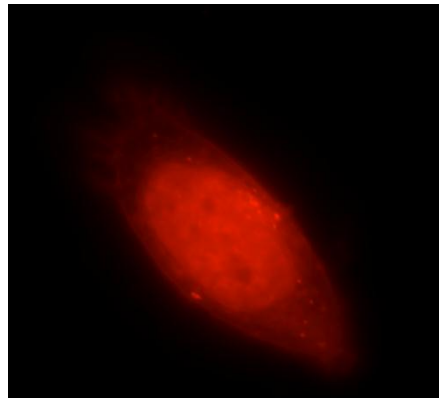
1 hour



6 hour



24 hour



48 hour

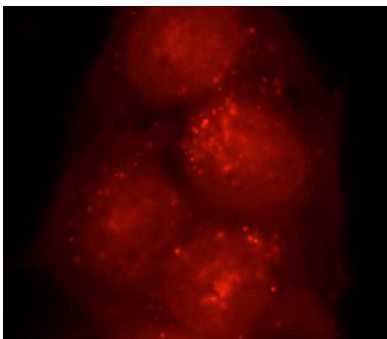
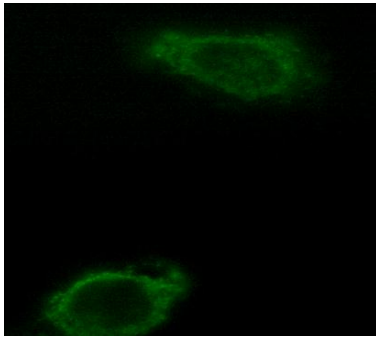


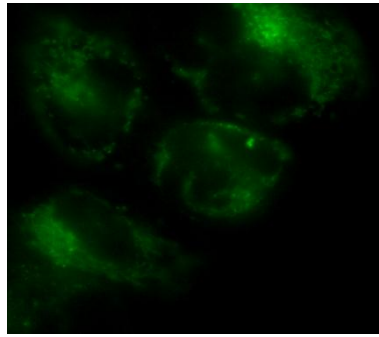
Figure 14:

Free Dox fluorescence micrograph of cells pretreated with 5 mg/mL HA for 24 hours.

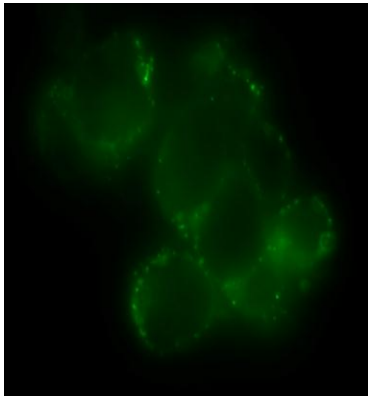
15 minute



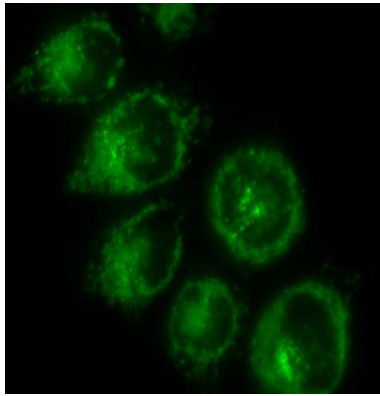
1 hour



6 hour



24 hour



48 hour

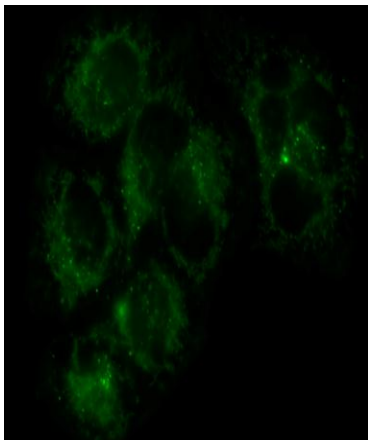
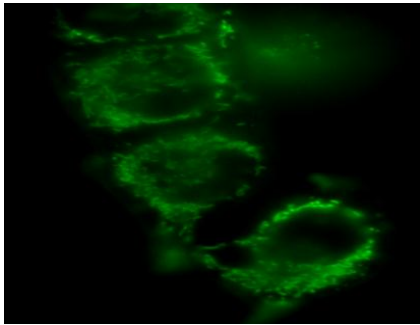


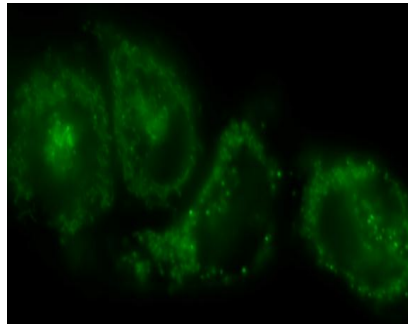
Figure 15:

HA-CY7 fluorescence micrograph of cells pretreated with 5 mg/mL HA for 24 hours.

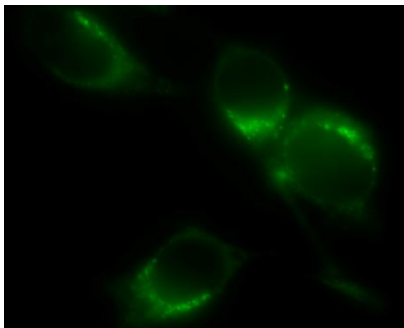
15 minute



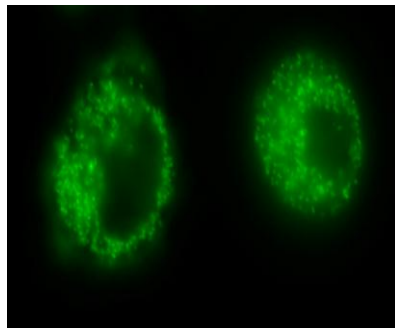
1 hour



6 hour



24 hour



48 hour

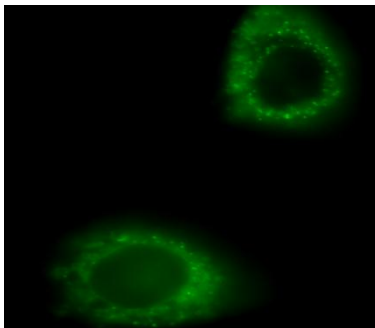
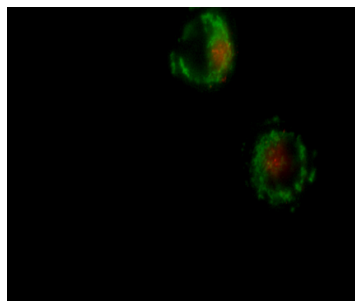


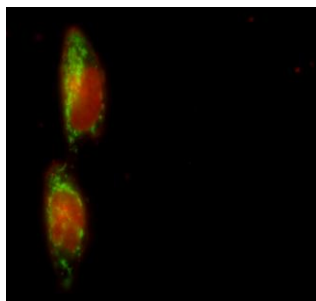
Figure 16:

Free CY7 fluorescence micrograph of cells pretreated with 5 mg/mL HA for 24 hours.

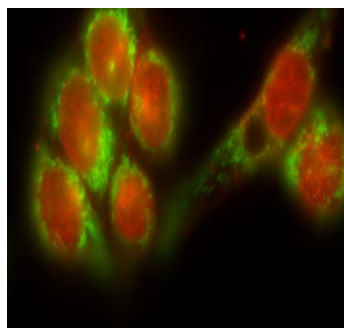
15 minute



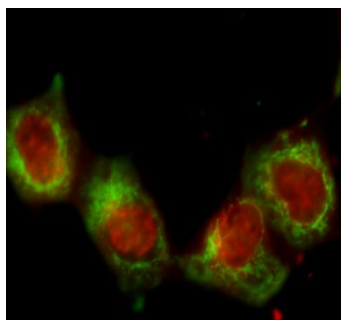
1 hour



6 hour



24 hour



48 hour

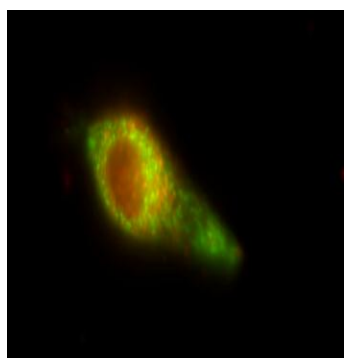
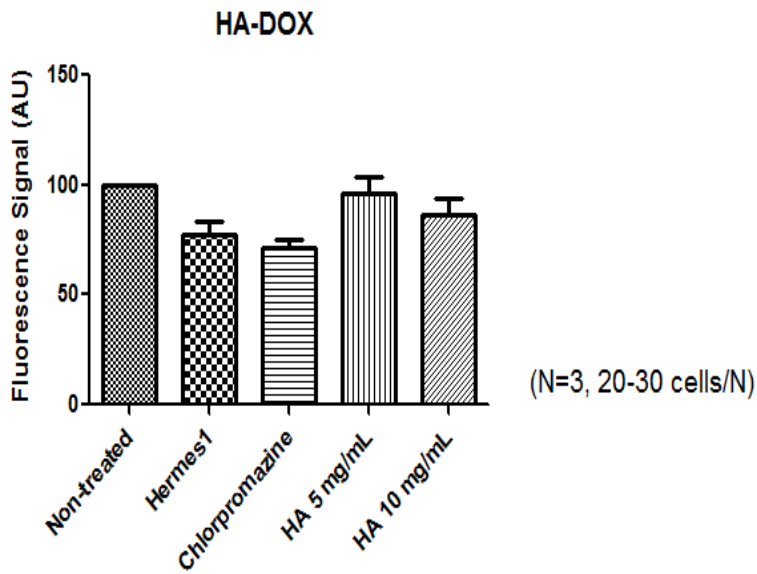


Figure 17:

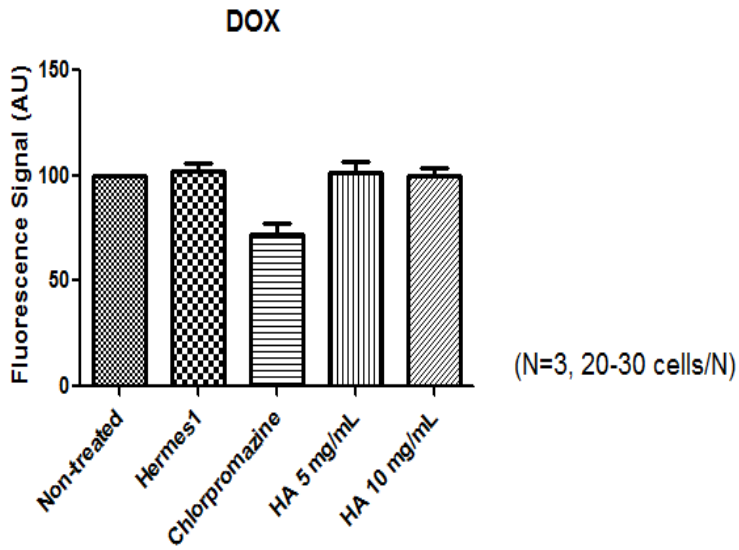
HA-DOX-CY7 fluorescence micrograph of cells pretreated with 5 mg/mL HA for 24 hours.



Treatment	P value
Non-treated vs. Hermes 1	0.0023
Non-treated vs. Chlorpromazine	0.0003
Non-treated vs. 5 mg/mL HA	0.4049
Non-treated vs. 10 mg/mL HA	0.0276

Figure 18:

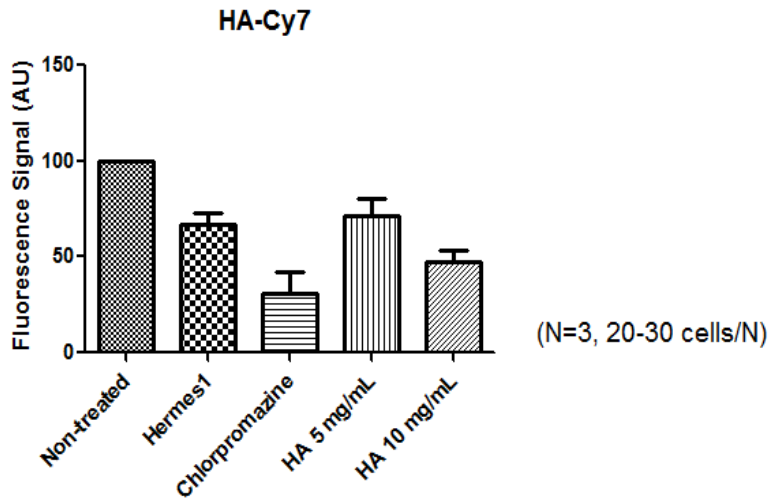
Comparison of cellular fluorescence intensity after one hour incubation with HA-DOX .



Treatment	P value
Non-treated vs. Hermes 1	0.4001
Non-treated vs. Chlorpromazine	0.0018
Non-treated vs. 5 mg/mL HA	0.6585
Non-treated vs. 10 mg/mL HA	0.9993

Figure 19:

Comparison of the cellular fluorescence intensity after one hour incubation with doxorubicin.



Treatment	P value
Non-treated vs. Hermes 1	0.0047
Non-treated vs. Chlorpromazine	0.0033
Non-treated vs. 5 mg/mL HA	0.0325
Non-treated vs. 10 mg/mL HA	0.0011

Figure 20:

Comparison of the cells fluorescence intensity after one hour incubation with HA-CY7.

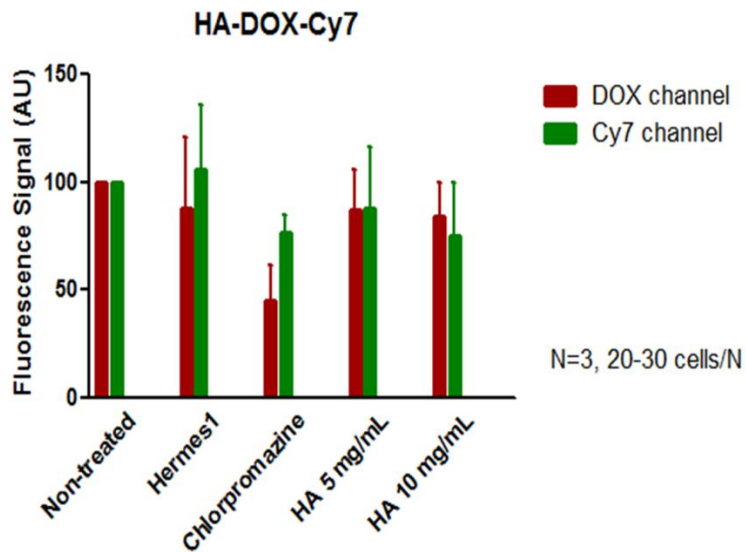


Figure 21:

Comparison of the cells fluorescence intensity after one hour incubation with HA-DOX-CY7

Cells treated with chlorpromazine had significant decrease of HA-DOX-CY7 uptake

(p value: < 0.05)

* CY7 signal

* DOX signal

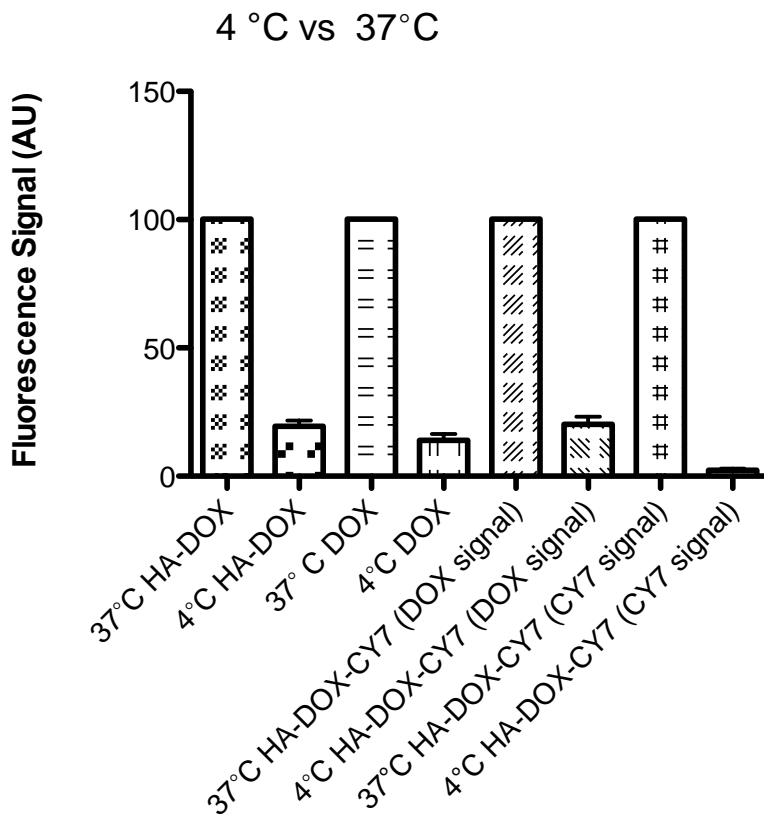


Figure 22:

Comparison of the cellular fluorescence intensity after one hour incubation with HA-DOX, DOX and HA-DOX-CY7 at 37°C and 4°C (p value less than 0.05 for all groups).

N=3,20-30 cells/N

2.5 Discussion:

We found that the uptake of HA-DOX and HA-CY7 conjugates was significantly decreased by the anti-CD44 antibody, Hermes-1, as well as by the presence of an excess of HA, suggesting that these conjugates enter the cell by a receptor-mediated process. CD44 is the primary cell surface receptor for HA, and it binds HA with five times greater affinity than the RHAMM (18). Excess HA also decreased the conjugates uptake, but the degree of inhibition was less than that by Hermes-1. This could be due to the more effective blocking by the monoclonal antibody Hermes-1. On the other hand, we cannot rule out the contribution of other HA receptors such as RHAMM in the HA-DOX conjugates uptake. RHAMM also has the capability to bind HA, although cell surface CD44 function is dominant (19). Also, DOX may have an effect on the cellular uptake of HA because the degree of the inhibition of HA-DOX uptake was less than that in HA-CY7.

Endocytosis is one of the basic cellular processes that is used by all cell types to internalize molecules by utilizing two different specialized proteins: clathrin and caveolin (20). Chlorpromazine, a specific inhibitor of clathrin-dependent endocytosis, significantly decreased the uptake of HA-DOX and HA-CY7 conjugates. These results suggest that HA-DOX and HA-CY7 conjugates are mainly internalized by the clathrin-mediated endocytosis pathway. Also, temperature-dependence study showed that the uptake of HA-DOX conjugates was significantly decreased at 4 °C, which further confirmed the endocytic pathway and that its entry is energy dependent.

On the other hand, the degradation pathway of NPs following internalization is another important aspect of intracellular NP dynamics. Degradation by lysosome is a common terminal destination for the endocytic pathway (21). We found that the lysosomes and HA-DOX conjugates were colocalized in the cytoplasm after 1 hour, suggesting that vesicles containing

the conjugates were migrated and fused with the lysosomes following the uptake. This result also further confirms the endocytic pathway of the conjugates in which the lysosomes is a common terminal destination of the endocytic pathway (22,23).

However, doxorubicin is a small hydrophobic molecule that could be internalized by passive diffusion. We found in this study that the uptake and cellular distribution of the DOX was decreased by chlorpromazine, a specific inhibitor of clathrin-dependent endocytosis, and by a temperature of 4°C. It has been suggested that the decrease in uptake of the DOX at 4°C compared to 37°C is due to the increase in the level of self-association of DOX and aggregation at 4°C by the formation of π -interaction (22,23). Also, the decrease in the DOX cellular uptake by chlorpromazine suggests the endocytic pathway of DOX. The uptake mechanism of DOX is not fully understood and needs further investigations.

We hypothesize that the conjugation of DOX to HA changes the uptake mechanism of DOX from passive diffusion to receptor mediated endocytosis process. The endocytosis process increases the retention time of DOX inside the cells and extends the release time of DOX from the conjugates.

2.6 Conclusion:

The suggested internalization mechanism of HA-DOX conjugates is an active transport mechanism mediated mainly by the CD44 receptor through a clathrin-dependent endocytic pathway. From the localization study, HA-CY7 distribution is in the cytosol and the free doxorubicin distribution is in the nucleus. This suggests that HA could not enter the nucleus, and HA-DOX conjugates enter the cell then release doxorubicin intracellularly. Lysosomes colocalized with HA-CY7, free doxorubicin, HA-DOX and HA-DOX-CY7 conjugates, so lysosomes could be the major degradation pathway of HA-DOX conjugates.

Chapter 3: Internalization of Sulfated-HA-CY7 experiments

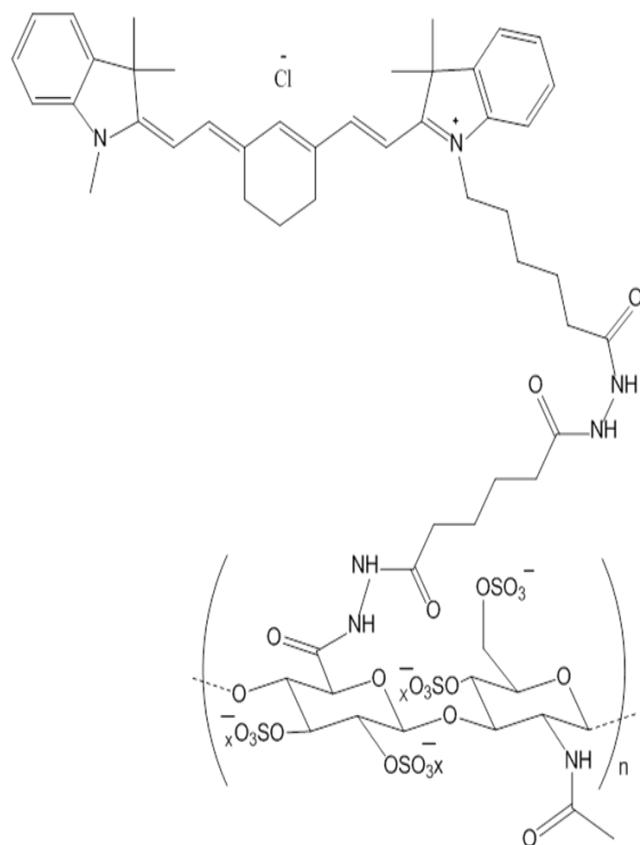


Figure 23: Chemical structure of Sulfated HA-ADH-CY7.

3.1 Method:

Cell line and cell culture condition:

The cell line used was a human head and neck squamous cell carcinoma cell line, MDA-1986. Cells were grown in 75-cm² cell culture flasks in DMEM with 10 % fetal bovine serum (FBS) and 1% glutamine. When a confluent state was reached, cells were seeded in 12-multiwell plates (100,000-200,000 cells/well). Before imaging the cells, they were washed three times with phosphate buffer saline (PBS). Then, the coverslips were fixed on glass microscope slides.

Uptake and cells tracking experiments:

The uptake of the sulfated HA was monitored by an inverted fluorescence microscope at 1 hour. To explore the mechanism of the sulfated-HA uptake and trafficking across the plasma membrane, we studied three different inhibition conditions.

Pathway	Inhibitor	Mechanism
HA receptor pathway	Hermes-1 (10 µg/mL)	Inhibits CD44-mediated uptake
HA receptor pathway	Excess HA (5 and 10 mg/mL)	Competitively inhibits HA uptake
Endocytosis	Chlorpromazine (25-µM)	Inhibits endocytosis by clathrin pathway

In chlorpromazine and Hermes-1 experiments, cells were incubated for 30 minutes with each inhibitor alone, and then co-incubated with Sulfated-HA-CY7 for 1 hour. In HA competition experiments, cells were treated with 10 mg/mL HA for 24 hours, and then co-incubated with sulfated HA for 1 hour. The fluorescence intensities for all three inhibition conditions were compared with non-treated cells using Image J program with this equation:

Corrected Total Cell Fluorescence (CTCF) = Integrated Density – (Area of selected cell X Mean fluorescence of background readings). Each assay was performed in triplicate and the statistical analysis was performed using student T test.

3.2 The results:

Sulfated HA-Cy7 has similar cellular distribution as the parent HA-CY7, and it is mainly localized in the cytosol (figure 24)

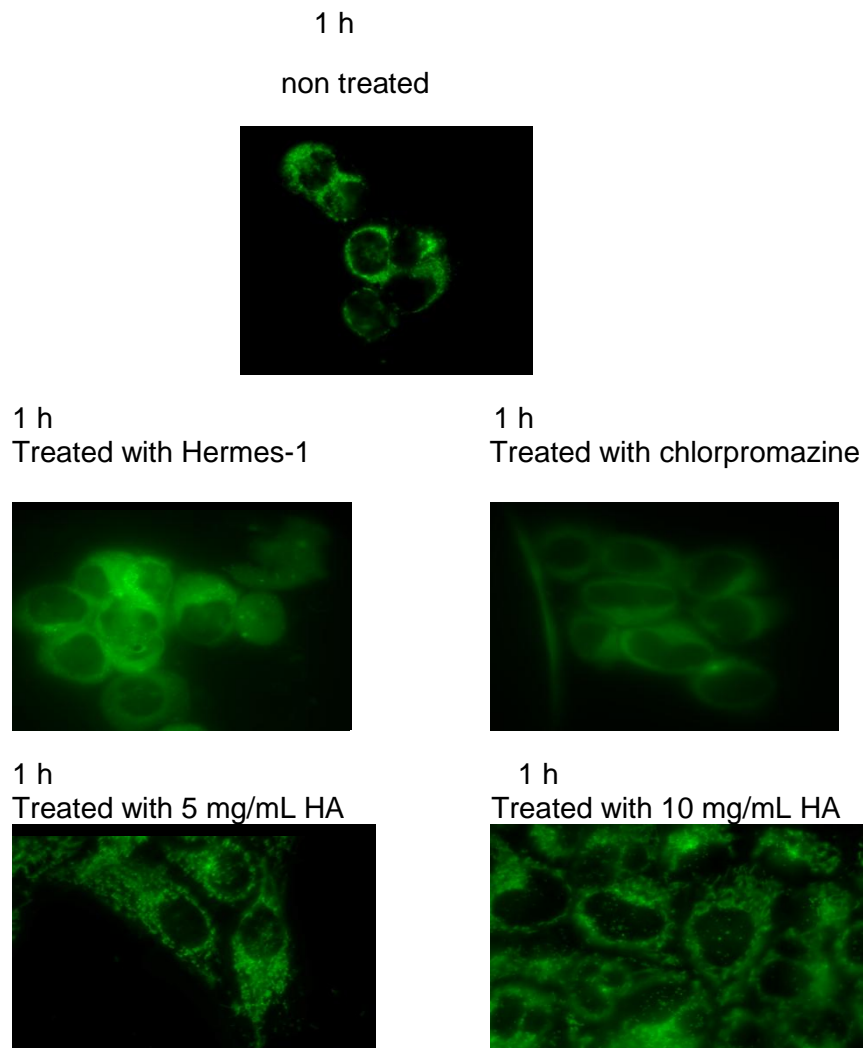


Figure 24:

Fluorescence micrographs of Sulfated-HA-CY7 (1 hour).

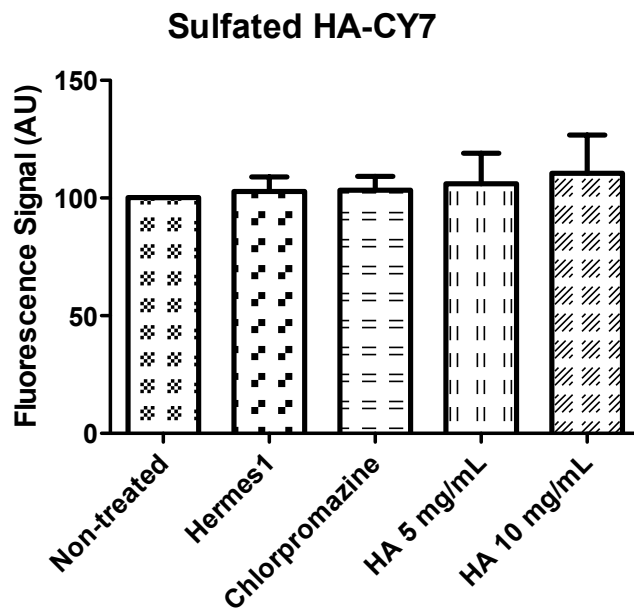


Figure 25: Comparison of the cellular fluorescence intensity after one hour incubation with Sulfated HA-CY7

N=3,20-30 cells/N

3.3 Discussion:

Hyaluronan was functionalized with a carboxylic functional group. We utilized this carboxylic functional group to conjugate HA to doxorubicin. However, this conjugation decreased the solubility of HA conjugates in the aqueous solution. Our lab derivitized the parent HA with a sulfate group to increase the solubility of the HA. In this work, we also compared the uptake of this sulfated form of HA to the parent HA. Sulfated HA can pass the cellular membrane, and it is mainly localized and distributed in the cytosol (figure 24). There is no effect of Hermes-1, chlorpromazine or excess HA on the uptake of the sulfated HA (figure 25). These results suggest that the uptake of sulfated HA is not dependent on the CD44 pathway, and the uptake could be by another mechanism such as passive diffusion or non-clathrin-mediated endocytosis.

Chapter 4:

Future work:

To explore the exact mechanism of the cellular uptake of HA-DOX and HA, we could try several blocking conditions such as: inhibiting energy dependent endocytosis processes; inhibiting ATP production; inhibiting caveoline-mediated endocytosis; inhibiting clathrin and caveolin-independent endocytosis pathways, macropinocytosis, and phagocytosis. Also, we could inhibit ATP production by incubating the cells with sodium azide 100-mM for 30 minutes before co-incubation of the cells with the nanoparticles. We could use metabolic inhibitors to inhibit the endocytosis such as colchicine (15-mM). Furthermore, we could specifically inhibit the caveoline-mediated endocytosis by incubating the cells with 1.25 µg/mL filipin for 30 minutes. Macropinocytosis is an actin-dependent endocytic mechanism mainly used by cells to internalize large amounts of fluids and growth factors. In contrast, phagocytosis is an endocytic mechanism used by cells to internalize solid particles, and it is also an actin-dependent process. To exclude the phagocytosis pathways we could try Vibrant™ Phagocytosis assay kit. We may not study the macro pinocytosis pathway because it involves internalization of relatively large particles (1–5 µm diameter), much larger than the HA-DOX conjugates (3).

We also could try different HA receptors blockers such as CD168 antibody to observe if they are involved in the uptake mechanism. Increasing the concentration of Hermes-1, chlorpromazine and HA in competitive experiment is another way to determine if the uptake is completely inhibited and if these mechanisms play a dominant role in HA-DOX uptake.

References:

1. Hillery, A., Lloyd, A., & Swarbrick, J. (Eds.) (2001). *Drug Delivery and Targeting*. Boca Raton: Taylor and Francis.
2. De Jong, W.H. & Borm, P.J. (2008). Drug delivery and nanoparticles: applications and hazards. *Int. J. Nanomedicine*, 3, 133-149.
3. Contreras-Ruiz, L., de la Fuente, M., Párraga, J., López-García, A., Fernández, I., Seijo, B., Sánchez, A., Calonge, M., Diebold, Y.(2011). Intracellular trafficking of hyaluronic acid-chitosan oligomer-based nanoparticles in cultured human ocular surface cells. *Mol. Vis*, 17,279-90.
4. Frasher, J.R.E et al, Laurent, T. C., Laurent, U. B. G. (1997) Hyaluronan: its nature, distribution, functions and turnover. *Journal of Internal Medicine*, 242 (1), 27–33.
5. Ouhtit, A., Abd Elmageed, Z., Abdraboh, M., Lioe, T., Raj, M. (2007).In vivo evidence for the role of CD44s in promoting breast cancer metastasis to the liver. *Am. J. Path.* 171,2033-2039.
6. Edetsberger, M., Gaubitzer, E., Valic, E., Waigmann, E., Köhler, G. (2005). Detection of nanometer-sized particles in living cells using modern fluorescence fluctuation methods. *Biochem Biophys Res Commun.*, 332,109–16.
7. Shenoy, D., Fu, W., Li, J., Crasto, C., Jones,G., DiMarzio,C., Sridhar,S., Amiji, M. (2006). Surface functionalization of gold nanoparticles using hetero-bifunctional poly (ethylene glycol) spacer for intracellular tracking and delivery. *Int. J. Nanomedicine*, 1, 51–7.
8. Panyam, J., Zhou, W.Z., Prabha, S., Sahoo, S., Labhasetwar, V. (2002).Rapid endo-lysosomal escape of poly (DL-lactide-co-glycolide) nanoparticles: implications for drug and gene delivery. *FASEB. J.*, 16, 1217–26.

9. Konan, Y.N., Chevallier, J., Gurny, R., Allémann, E. (2003). Encapsulation of p-THPP into nanoparticles: cellular uptake, subcellular localization and effect of serum on photodynamic activity. *Photochem. Photobiol.*, 77, 638–44.
10. Cai, S., Thati, S., Bagby, T., Diab, H., Davies, N., Cohen, M., & Forrest, L. (2010). Localized doxorubicin chemotherapy with a biopolymeric nanocarrier improves. *J. Control. Rel.*, 146, 212–218.
11. Luo, Y., Prestwich, G.D. (1999). Synthesis and selective cytotoxicity of a hyaluronic acid antitumor bioconjugate, *Bioconjug. Chem.*, 10 (5), 755–763.
12. Bouhadir, K.H., Alsberg, E., Mooney, D.J. (2001). Hydrogels for combination delivery of antineoplastic agents, *Biomaterials*, 22 (19) 2625–2633.
13. Cai, S. (2010). Internalization of Nanocarriers into Tumor Cells. Unpublished doctoral dissertation, University of Kansas.
14. Sugahara, S., Okuno, S., Yano, T., Hamana, H., Inoue, K. (2001). Characteristics of tissue distribution of various polysaccharides as drug carriers: influences of molecular weight and anionic charge on tumor targeting, *Biol. Pharm. Bull.* 24 (5) 535–543.
15. Cera, C., Palumbo, M., Stefanelli, S., Rassa, M., Palù, G. (1992). Water-soluble polysaccharide-anthracycline conjugates: biological activity, *Anticancer Drug Des.* 7 (2) 143–151.
16. Akima, K., Ito, H., Iwata, Y., Matsuo, K., Watari, N., Yanagi, M., Hagi, H., Oshima, K., Yagita, A., Atomi, Y., Tatekawa, I. (1996). Evaluation of antitumor activities of hyaluronate binding antitumor drugs: synthesis, characterization and antitumor activity, *J. Drug Target.* 4 (1) 1–8.
17. Takemura, G., Fujiwara, H. (2007). Doxorubicin-induced cardiomyopathy from the cardiotoxic mechanisms to management, *Prog. Cardiovasc. Dis.* 49 (5) 330–352.

18. Sherman, L., Sleeman, J., Herrlich, P., Ponta, H. (1994). Hyaluronate receptors: key players in growth, differentiation, migration and tumor progression. *Curr. Opin. Cell. Biol.*; 6:726-33.
19. Nedvetzki, S., Gonen, E., Assayag, N., Reich, R., Williams, RO., Thurmond, RL., Huang, JF., Neudecker, BA., Wang, FS., Turley, EA., Naor, D. (2004). RHAMM, a receptor for hyaluronan-mediated motility, compensates for CD44 in inflamed CD44-knockout mice: a different interpretation of redundancy. *Proc. Natl. Acad. Sci. USA*; 101:18081-6.
20. Mayor, S., Pagano, RE. (2007). Pathways of clathrin-independent endocytosis. *Nat. Rev. Mol. Cell Biol.*; 8:603-12.
21. Van ME, Klumperman, J. (2008). Imaging and imagination: understanding the endo-lysosomal system. *Histochem. Cell. Biol.*; 129:253-66.
22. Dalmark, M., Storm, H. (1981). A Fickian diffusion process with features of transport catalysis. Doxorubicin transport in Human red blood cells. *J. Gen. Physiol*, 78,349-364.
23. Majumdar, S., Kobayashi, N., Krise, JP., Siahaan, TJ. (2007). Mechanism of internalization of an ICAM-1-derived peptide by human leukemic cell line HL-60: influence of physicochemical properties on targeted drug delivery. *Mol. Pharm.*, Sep-Oct; 4(5):749-58.